Cell Death and Differentiation (2014) 21, 1709–1720

www.nature.com/cdd

Distinct roles of RIP1–RIP3 hetero- and RIP3–RIP3 homo-interaction in mediating necroptosis

X-N Wu[1,2], Z-H Yang[1,2], X-K Wang[1], Y Zhang[1], H Wan[1], Y Song[1], X Chen[1], J Shao[1] and J Han*[,1]

Necroptosis is mediated by a signaling complex called necrosome, containing receptor-interacting protein (RIP)1, RIP3, and mixed-lineage kinase domain-like (MLKL). It is known that RIP1 and RIP3 form heterodimeric filamentous scaffold in necrosomes through their RIP homotypic interaction motif (RHIM) domain-mediated oligomerization, but the signaling events based on this scaffold has not been fully addressed. By using inducible dimer systems we found that RIP1–RIP1 interaction is dispensable for necroptosis; RIP1–RIP3 interaction is required for necroptosis signaling, but there is no necroptosis if no additional RIP3 protein is recruited to the RIP1–RIP3 heterodimer, and the interaction with RIP1 promotes the RIP3 to recruit other RIP3; RIP3–RIP3 interaction is required for necroptosis and RIP3–RIP3 dimerization is sufficient to induce necroptosis; and RIP3 dimer-induced necroptosis requires MLKL. We further show that RIP3 oligomer is not more potent than RIP3 dimer in triggering necroptosis, suggesting that RIP3 homo-interaction in the complex, rather than whether RIP3 has formed homo polymer, is important for necroptosis. RIP3 dimerization leads to RIP3 intramolecule autophosphorylation, which is required for the recruitment of MLKL. Interestingly, phosphorylation of one of RIP3 in the dimer is sufficient to induce necroptosis. As RIP1–RIP3 heterodimer itself cannot induce necroptosis, the RIP1–RIP3 heterodimeric amyloid fibril is unlikely to directly propagate necroptosis. We propose that the signaling events after the RIP1–RIP3 amyloid complex assembly are the recruitment of free RIP3 by the RIP3 in the amyloid scaffold followed by autophosphorylation of RIP3 and subsequent recruitment of MLKL by RIP3 to execute necroptosis.
Cell Death and Differentiation (2014) **21,** 1709–1720; doi:10.1038/cdd.2014.77; published online 6 June 2014

Necroptosis is a type of programmed necrosis characterized by necrotic morphological changes, including cellular organelle swelling, cell membrane rupture,[1–3] and dependence of receptor-interacting protein (RIP)1[4] and RIP3.[5–7] Physiological function of necroptosis has been illustrated in host defense,[8–11] inflammation,[12–16] tissue injury,[10,17,18] and development.[19–21]

Necroptosis can be induced by a number of different extracellular stimuli such as tumor necrosis factor (TNF). TNF stimulation leads to formation of TNF receptor 1 (TNFR1) signaling complex (named complex I), and complex II containing RIP1, TRADD, FAS-associated protein with a death domain (FADD), and caspase-8, of which the activation initiates apoptosis. If cells have high level of RIP3, RIP1 recruits RIP3 to form necrosome containing FADD,[22–24] caspase-8, RIP1, and RIP3, and the cells undergo necroptosis.[25,26] Caspase-8 and FADD negatively regulates necroptosis,[27–30] because RIP1, RIP3, and CYLD are potential substrates of caspase-8.[31–34] Necrosome also suppresses apoptosis but the underlying mechanism has not been described yet. Mixed-lineage kinase domain-like (MLKL) is downstream of RIP3,[35,36] and phosphorylation of MLKL is required for necroptosis.[37–42]

Apoptosis inducing complex (complex II) and necrosome are both supramolecular complexes.[43–45] A recent study showed that RIP1 and RIP3 form amyloidal fibrils through their RIP homotypic interaction motif[46] (RHIM)-mediated polymerization, and suggested that amyloidal structure is essential for necroptosis signaling.[47] The RIP1–RIP3 heterodimeric amyloid complex is believed to function as a scaffold that brings signaling proteins into proximity to permit their activation. However, RIP1 and RIP3 also can each form fibrils on their own RHIM domains *in vitro*. It is unclear how the homo- and hetero-interactions are coordinated and organized on the amyloid scaffold to execute their functions in necroptosis. Here, we used inducible dimerization systems to study the roles of RIP1–RIP1, RIP1–RIP3, and RIP3–RIP3 interactions in necroptosis signaling. Our data suggested that it is the RIP1–RIP3 interaction in the RIP1–RIP3 heterodimeric amyloid complex that empowers to recruit other free RIP3; homodimerization of RIP3 triggers its autophosphorylation and only the phosphorylated RIP3 can recruit MLKL to execute necroptosis.

Results

Domains in RIP1 that control dimerization or polymerization and their role in necroptosis and apoptosis. RIP1 contains a kinase domain, an RHIM domain, and a death domain (DD) (Figure 1a).[48] As dimerization or polymerization

[1]State Key Laboratory of Cellular Stress Biology, Innovation Center for Cell Biology, School of Life Sciences, Xiamen University, Xiamen, Fujian, China
*Corresponding author: J Han, State Key Laboratory of Cellular Stress Biology, Innovation Center for Cell Biology, School of Life Sciences, Xiamen University, Xiamen, Fujian, China. Tel: +86 592 2187680; Fax: +86 592 2187930; E-mail: jhan@xmu.edu.cn or jhan@scripps.edu
[2]These authors are the joint first authors.
Abbreviations: RIP3, receptor-interacting protein 3; MLKL, mixed-linage kinase domain-like; TNF, tumor necrosis factor; TNFR1, TNF receptor 1; FADD, FAS-associated protein with a death domain; RHIM, RIP homotypic interaction motif; DD, death domain; Nec-1, necrostatin-1; zVAD, Z-Val-Ala-DL-Asp-fluoromethylketone; DSS, disuccinimidyl suberate
Received 13.12.13; revised 02.4.14; accepted 23.4.14; Edited by G Melino; published online 06.6.14

of RIP1 is considered to be involved in TNF-induced necroptosis and/or apoptosis,[49] we first evaluated the contributions of these domains to the interaction between RIP1 proteins. HA-RIP1 mutants (Figure 1a) were co-expressed with or without Flag-tagged full-length RIP1 in 293T cells and their interaction was determined by co-immunoprecipitation (Figure 1b). The results showed that both RHIM and DD were capable of mediating the interaction between RIP1 proteins (Figure 1b).

Total internal reflection fluorescence microscopy, combined with the conventional pull-down assay with a single molecule, enables direct visualization of individual protein complex from the cell extract.[50] We use this method to determine the potential of DD and RHIM domain in forming dimers or polymers. We expressed Flag-RFP-tagged DD or RHIM domain of RIP1 in 293T cells and prepared a flow chamber covered with anti-Flag antibody.[50] The immunoprecipitated complexes of DD and RHIM domain were visualized through RFP (Figures 1c and d). Applying a defined continuous laser power to these complexes could induce stepwise loss of fluorescence,[50] thereby obtaining stoichiometric information. The distribution of photobleaching steps of DD was binomial (Figures 1e and f), suggesting that DD of RIP1 prefers to form dimer. Meanwhile, the analysis of RHIM revealed bright fluorescent spots (Figure 1d) and unresolved bleaching steps (Figure 1g), suggesting RIP1's RHIM domain

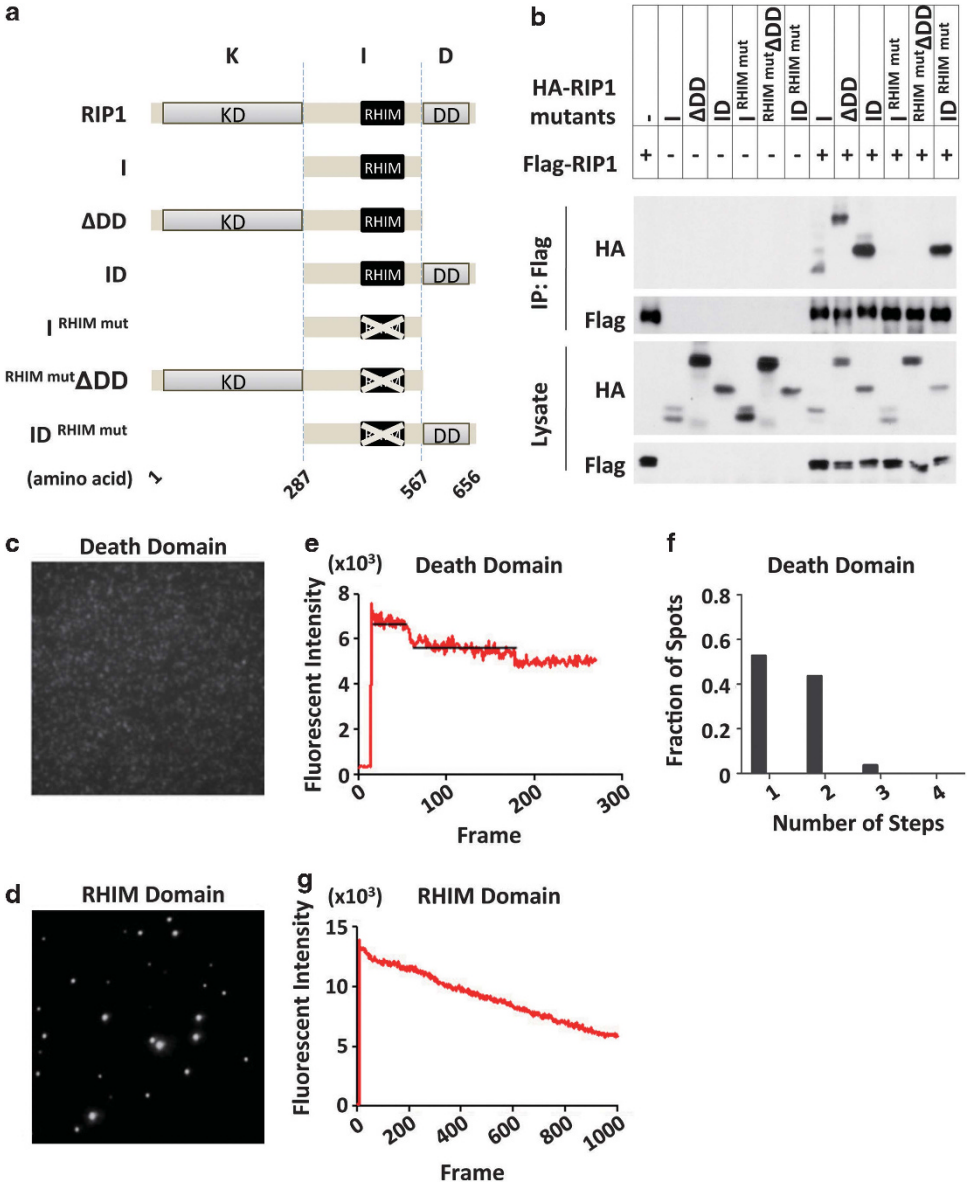

Figure 1 The RHIM and DD domains are both capable of mediating the interaction of RIP1 proteins. (**a**) Schematic representation of murine RIP1 and its truncations. K, I, and D represent the kinase domain, intermediate sequence, and DD of RIP1, respectively. RHIM mut represents QIG529–531AAA mutation on the RHIM in RIP1. The amino acid number is indicated. (**b**) Flag-RIP1 was co-transfected with HA-RIP1 mutants in 293T cells. Thirty-six hours post transfection, cell lysates were immunoprecipitated with anti-Flag antibody. The cell lysates and immunoprecipitates were analyzed by western blotting. (**c** and **d**) Total internal reflection fluorescence (TIRF) of Flag-RFP-tagged DD (**c**) or RHIM domain (**d**). (**e**–**g**) Photobleaching step distribution for Flag-RFP-tagged DD (**e** and **f**) and RHIM domain (**g**)

potentially contributes to polymerization, as is consistent with a recent report indicating RHIM forms amyloidal complex.[47]

As RIP1 is involved in necroptosis and apoptosis,[48] we checked the requirement of its RHIM and DD in cell death. According to previous reports, pan-caspase inhibitor Z-Val-Ala-DL-Asp-fluoromethylketone (zVAD) was used to distinguish apoptosis from necroptosis.[6] RIP1 mutants were overexpressed in *Rip1*$^{-/-}$*Rip3*^{d} MEF, which lacks the expression of RIP1 and RIP3 (Zhang *et al.*[5]; Figure 2a). As reported, overexpression of full-length RIP1 leads to caspase-dependent cell death (apoptosis) in *Rip1*$^{-/-}$*Rip3*^{d} MEFs and caspase-independent cell death (necroptosis) in *Rip1*$^{-/-}$*Rip3** MEFs, in which RIP3 expression is reconstituted (Figure 2a). Deletion of DD (ΔDD) abolished its ability to induce apoptosis but not necroptosis (Figure 2a). Overexpression of RIP1$^{RHIM\ mut}$ΔDD, the RIP1 with ΔDD plus RHIM^{mut}, could not cause RIP3-dependent necroptosis (Figure 2a). These data demonstrated that the DD domain of RIP1 is required for apoptosis, while the RHIM domain is required for necroptosis.

RIP1–RIP1 interaction is dispensable for necroptosis. RIP1's RHIM domain mediates RIP1–RIP1 and RIP1–RIP3 interaction. To determine whether the loss of function of RIP1$^{RHIM\ mut}$ in necroptosis is due to defect in either RIP1–RIP1 interaction or RIP1–RIP3 interaction, or both, we constructed RIP1 and RIP3 into a heterodimer expressing system. In brief, we fused RIP1$^{RHIM\ mut}$, RIP1$^{RHIM\ mut}$ΔDD, and RIP3^{WT} with two heterodimer adaptors, which are FKBP (FK506-binding protein) and FRB* (domain of mTOR with a point mutation T2098L), as indicated (Figure 2b). The interaction of FKBP and FRB* can be induced by a rapamycin analog AP21976.[51] The RHIM domain in RIP1 was mutated to ensure the inducible interaction is RHIM independent.

Overexpression of FKBP-RIP1$^{RHIM\ mut}$ or FRB*-RIP1$^{RHIM\ mut}$ caused apoptosis in *Rip1*$^{-/-}$*Rip3*^{d} MEFs, and this apoptosis could be abolished by DD deletion and slightly reduced by necrostatin-1 (Nec-1), whereas overexpression of FRB*-RIP3^{WT} caused necroptosis (Supplementary Figure S1a and b). By controlling the titer of lentiviral vectors and selecting the live cells, the overexpression effect was avoided and the expression levels of these FKBP or FRB fusion proteins were lower than their endogenous counterparts (Figure 2c). We then treated these cells with or without AP21967 to study the effect of the dimerization of given RIP1 or RIP3 mutants in *Rip1*$^{-/-}$*Rip3*^{d} MEFs. The results demonstrated that AP21967 had no effect on viability of the cells expressing any of these proteins alone (Figure 2c). AP21967 induced death in cells expressing FKBP-RIP1$^{RHIM\ mut}$ plus FRB*-RIP3^{WT} (Figure 2c), demonstrating the role of RIP1–RIP3 interaction in necroptosis. To exclude the possibility that DD-mediated interaction between RIP1$^{RHIM\ mut}$ proteins has a role in AP21967-induced cell death, we co-expressed FKBP-RIP1$^{RHIM\ mut}$ΔDD with FRB*-RIP3^{WT} and found AP21967 induced the same level of death in these cells as compared with the cells expressing FKBP-RIP1$^{RHIM\ mut}$ with FRB*-RIP3^{WT}; we co-expressed FKBP-RIP1$^{RHIM\ mut}$ΔDD with FRB*-RIP1$^{RHIM\ mut}$ΔDD and did not detect any cells death after AP21967 treatment (Figure 2c). Thus, RIP1–RIP3 interaction is required for necroptosis while RIP1–RIP1 is dispensable.

The RIP1–RIP3 heterodimer itself cannot initiate necroptosis. As the RIP3, in RIP1$^{RHIM\ mut}$-RIP3^{WT} complex, could interact with other RIP3 via its intact RHIM domain, we next determined whether this RHIM domain is required for RIP1$^{RHIM\ mut}$-RIP3^{WT}-induced necroptosis (Figure 2c). We co-expressed FRB*-RIP3$^{RHIM\ mut}$ (Figure 2d), whose interaction with another RIP3 was disrupted by mutations in RHIM (Supplementary Figure S2a), with FKBP-RIP1$^{RHIM\ mut}$ in *Rip1*$^{-/-}$*Rip3*^{d} MEFs. Indeed, addition of AP21967 did not induce cell death in the cells expressing both FKBP-RIP1$^{RHIM\ mut}$ and FRB*-RIP3 $^{RHIM\ mut}$ (Figure 2d), indicating that RIP1–RIP3 heterodimer itself cannot induce necroptosis.

Recruitment of additional RIP3 proteins to RIP1–RIP3 heterodimer causes necroptosis. As the inducible interaction of RIP1$^{RHIM\ mut}$-RIP3^{WT}, but not RIP1$^{RHIM\ mut}$-RIP3$^{RHIM\ mut}$, caused necroptosis (Figure 2d), we reasoned that RIP3^{WT} interacts with other RIP3 through its RHIM during AP21967 treatment. To test this, we first performed co-immunoprecipitation and found that AP21967 induced dimerization of RIP1$^{RHIM\ mut}$-RIP3$^{RHIM\ mut}$, as well as RIP1$^{RHIM\ mut}$-RIP3^{WT} (Figure 2e). We noticed a band shift of exogenously expressed wild-type (WT) RIP3, which should be resulted from T257 phosphoryation.[52] The T257 phosphorylation of RIP3 is not involved in necroptosis but why it requires RHIM domain is unclear.

Next, we analyzed whether FRB*-RIP3^{WT} in the RIP1$^{RHIM\ mut}$-RIP3^{WT} heterodimer is able to interact with other RIP3, by including another HA-RIP3, as we were unable to determine whether there was another FRB*-RIP3 in complex. Additional low level of HA-RIP3 did not change the profile of cell death in response to AP21967 (Figure 2f). From the cells co-expressing FKBP-RIP1 $^{RHIM\ mut}$, FRB*-RIP3^{WT}, and HA-RIP3, we found that HA-RIP3 only interacted with AP21976-induced RIP1$^{RHIM\ mut}$–RIP3^{WT} complex, but not RIP1$^{RHIM\ mut}$–RIP3$^{RHIM\ mut}$ complex (Figure 2g), thereby suggesting that inducible RIP1–RIP3 heterodimer could recruit another RIP3 protein and this recruitment may be required for necroptosis. Caspase-8 is known to inhibit necroptosis[19,20,31] and zVAD indeed tended to increase the cell death induced by RIP1–RIP3 complex, although the enhancement is not always statistically significant (Figures 2c, d and f). The participation of caspase-8 in RIP1–RIP3 dimer-induced cell death was supported by the data that caspase-8 can be detected in AP21967-induced RIP1–RIP3 complex (Supplementary Figure S2d).

RIP3–RIP3 homodimerization is sufficient to trigger MLKL-dependent necroptosis. As RIP1–RIP3 heterodimer needs additional RIP3 protein(s) for necroptosis signaling (Figures 2f and g), we further investigated whether RIP3 dimerization is sufficient to induce necroptosis. After confirming the AP21967-induced FKBP-RIP3$^{RHIM\ mut}$ and FRB*-RIP3$^{RHIM\ mut}$ interaction in 293T cells (Figure 2b and Supplementary Figure S2b), we co-expressed these two proteins in WT and *Rip1*$^{-/-}$*Rip3*^{d} MEF cells, and examined cell death. The results showed that AP21967 effectively induced necroptosis in cells expressing both proteins, but not any of them alone (Supplementary Figures S2c and 3a), indicating that RIP3 homodimer but not monomer induces

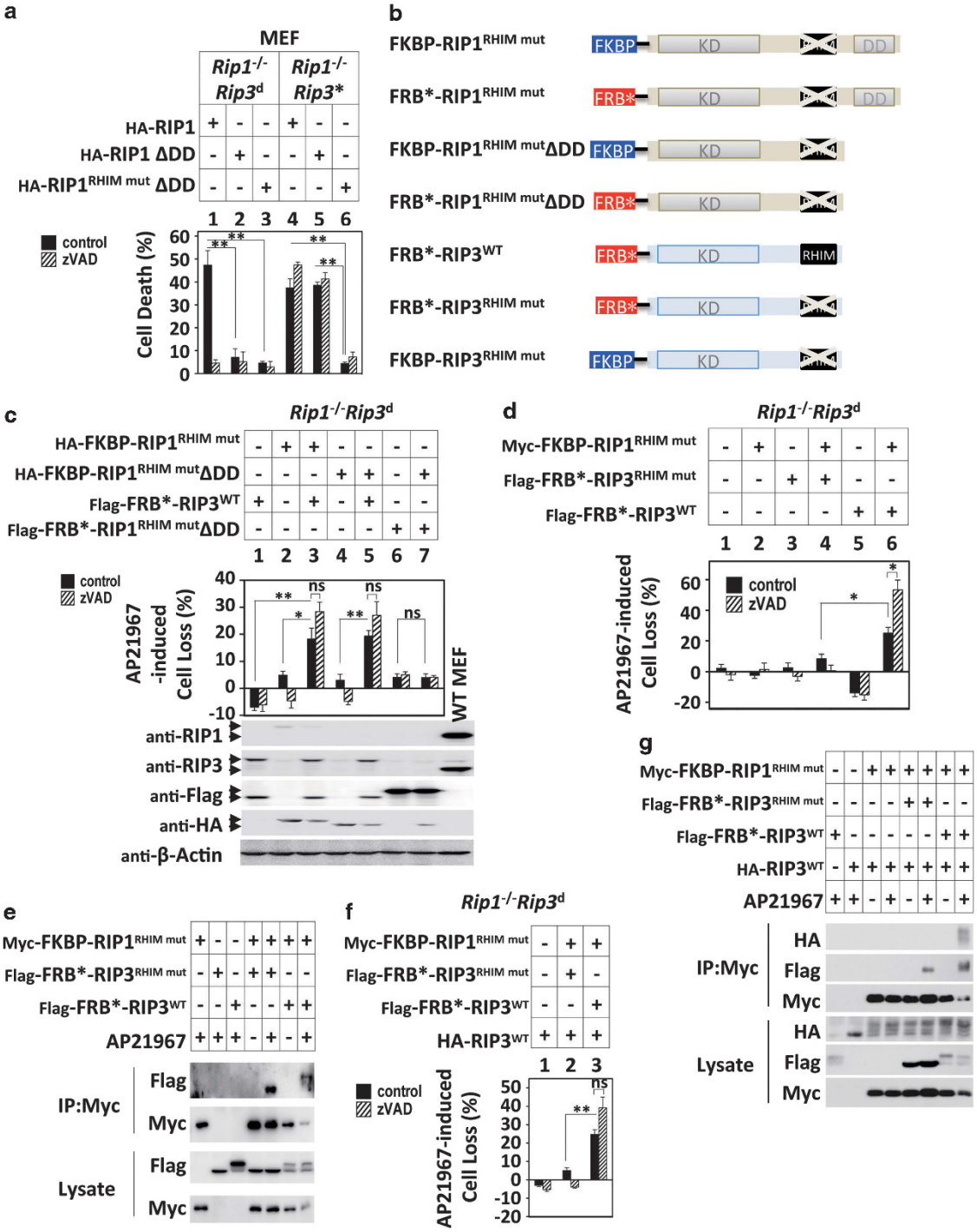

Figure 2 The RIP1–RIP3 heterodimer itself cannot initiate necroptosis, but recruitment of additional RIP3 protein(s) to this heterodimer causes necroptosis. (**a**) *Rip1*$^{-/-}$ *Rip3*^{d} and *Rip1*$^{-/-}$ *Rip3** MEF cells were infected with lentivirus encoding the RIP1 variants as indicated, cultured with or without zVAD (20 μM). Thirty hours after infection, cell death assay was performed using propidium iodide (PI) exclusion. (**b**) Schematic representation of the heterodimer adaptors (FKBP and FRB*) fused RIP1 and RIP3 variants. RHIM mut in RIP3 represents QIG449–451AAA mutation in RHIM domain. (**c**, **d** and **f**) *Rip1*$^{-/-}$ *Rip3*^{d} MEF cells were infected with lentivirus as indicated, followed by the heterodimerizer AP21967 treatment (250 nM), with or without zVAD (20 μM). Cell loss was determined by ATP levels. (**e** and **g**) 293T cells were transfected with the indicated constructs. After 36 h, these cells were treated with mock or AP21967 (250 nM) for 1 h, followed by immunoprecipitation with anti-Myc antibody and subsequent western blotting analysis. All data above were represented as mean ± S.E.M. of three independent experiments. *$P<0.05$. **<0.01. n.s., nonsignificant

necroptosis and this is RIP1 independent. We also used another dimerization system based on estrogen-induced homodimerization of hormone-binding domain (HBD) of estrogen receptor. To avoid the effect of serum estrogen, HBD*, a mutated HBD (G521R) that binds to a synthetic anti-estrogen 4-hydroxytamoxifen (4-OHT) more effectively

than estrogen,[53] was used in our experiments. The HBD* was fused to either N- or C-terminal of RIP3 $^{RHIM\ mut}$ (Supplementary Figure S3a). The HBD*-RIP3$^{RHIM\ mut}$ and RIP3$^{RHIM\ mut}$-HBD* were introduced into *Rip1*$^{-/-}$ *Rip3*^{d} MEF cells or L929 cells, respectively. Consistently, cell death was induced by 4-OHT in cells expressing HBD*-RIP3$^{RHIM\ mut}$ (Supplementary Figures S3b and c). However, 4-OHT did not induce death in the cells expressing RIP3$^{RHIM\ mut}$-HBD* (Supplementary Figure S3b). It is possible that the fusion of HBD* to C-terminal of RIP3 interferes with its function. Using RIP3 with C-terminal fusion of a dimerization domain to study the effect of RIP3 dimerization on cell death was recently reported[54,55] and Orozco *et al*., submitted). They showed that C-terminus-mediated dimerization of RIP3Δ^{RHIM} could not induce necroptosis, which is in line with our observation. Nonetheless, our data demonstrated that dimerization of RIP3 is sufficient to trigger necroptosis.

To determine whether RIP3 homodimer-induced necroptosis is MLKL-dependent, we stably expressed FKBP-RIP3$^{RHIM\ mut}$ and FRB*-RIP3$^{RHIM\ mut}$ in *Mlkl* knockout (KO) L929 cells, while *Rip3* KO L929 was used as control. We found that RIP3 homodimerization could not induce necroptosis when *Mlkl* was deleted, while in contrast, it effectively induced necroptosis in *Rip3* KO cells (Figure 3b). Neither zVAD nor RIP1 kinase inhibitor Nec-1 inhibited RIP3 homodimer-induced necroptosis (Figure 3c), confirming that RIP3 dimer-induced necroptosis does not require RIP1 and is caspase independent. Taken together, these data demonstrated that similar to TNF-induced necroptosis, RIP3 homodimer-induced necroptosis requires MLKL.

To ensure that the necroptosis referred above was indeed induced by RIP3 dimer but not polymer, we performed size-exclusion chromatography to fractionate lysates from control and AP21967-treated cells expressing HA-FKBP-RIP3$^{RHIM\ mut}$ and Flag-FRB*-RIP3$^{RHIM\ mut}$, and both *Rip3* KO and *Mlkl* KO L929 cells were used. To determine which fractions are rich of the RIP3 dimer, we immunoprecipitated Flag-FRB*-RIP3$^{RHIM\ mut}$ from each column fractions. The co-immunoprecipitation showed that AP21967-induced complex was present in the fractions 15–16 with molecular mass of 158–440 kDa (Figure 3d), while this complex could not be detected in mock-treated cells, and the results are similar in *Rip3* KO and *Mlkl* KO cells (Figure 3d).

To analyze the size of TNF-induced endogenous RIP1/RIP3 complex for comparison, we used a L929 cell line, in which a Flag tag coding sequence was inserted into the *RIP3* gene to express C-terminal Flag-tagged RIP3 and it behaves the same as WT L929. The co-immunoprecipitation showed that RIP1 interacted with Flag-tagged RIP3 in the fractions 9–10 (Figure 3e), as is consistent with published results that RIP1/RIP3 complex is about 2 MDa.[43,44] These data confirmed that the size of AP21967-induced RIP3 complex is different from TNF-induced RIP1/RIP3 complex.

To further determine the exact size of AP21967-induced RIP3 complex, we cross-linked proteins with disuccinimidyl suberate (DSS) and immunoprecipitated Flag-FRB*-RIP3$^{RHIM\ mut}$. Western blotting of the Flag immunoprecipitates with anti-HA antibody revealed an AP21967-induced complex with a molecular mass between 130 and 170 kDa (Figure 3f). As the molecular masses of HA-FKBP-RIP3$^{RHIM\ mut}$ and Flag-FRB*-RIP3$^{RHIM\ mut}$ are 75 and 70 kDa, respectively, AP21967 indeed induced dimerization of RIP3. It needs to note that we did not see a band between 130 and 170 kDa in the western analysis of Flag immunoprecipitates by anti-flag antibody, which is most likely due to that the Flag immunoprecipitates containing all kinds of cross-linked Flag-FRB*-RIP3, which overwhelmed the signal of Flag-RIP3 in the HA-FKBP-RIP3$^{RHIM\ mut}$ and Flag-FRB*-RIP3$^{RHIM\ mut}$ dimers. DSS appears to have cross-linked a large number of different proteins, as the monomers of HA- and Flag-tagged proteins were dramatically reduced after DSS treatment (Figure 3f). Another note is that we only can detect RIP3 dimer but not RIP3-MLKL complex in the cross-linking experiments, which might be due to that RIP3-MLKL complex is less abundant than AP-induced RIP3 dimer and also could be heterogenous.

Oligomerization of RIP3 is not more potent than dimerization in generating necroptosis signaling. TNF-induced necrosome complex is mega Dalton in size[43–45] and a fibrillar core structure of RIP1–RIP3 complex in cells has been observed.[47] As RIP1–RIP3 interaction itself cannot trigger necroptosis, there must be RIP3–RIP3 homodimeric or oligomeric interaction in necrosome for necroptosis signaling. As RIP3 itself can form amyloidal oligomers *in vitro*,[47] we sought to determine whether there is a difference in necroptosis signaling if dimer or oligomer of RIP3 was formed. To address this, we first examined whether FKBP-RIP3^{WT} and FRB*-RIP3$^{RHIM\ mut}$ complex contains multiple RIP3, as RHIM is responsible for oligomerization.[47] We co-expressed both proteins in L929 cells and analyzed AP21967-induced RIP3 complexes by size-exclusion chromatography (Figure 4a). We detected that RIP3 dimer complex formed by RIP3^{WT}-RIP3$^{RHIM\ mut}$ mainly in fractions 13–16, and that a small portion of complex containing RIP3^{WT}-RIP3$^{RHIM\ mut}$ as well as endogenous RIP3 in fractions 7–10 with molecular mass of 2 MDa, indicating that AP21967 induced a complex containing multiple RIP3 (Figure 4a). The amount of RIP3 in the 2 MDa complex is $\sim$10% of that in dimer complex based on the measurement of HA and endogenous RIP3 (Figure 4a). We then co-expressed Flag-FRB*-RIP3$^{RHIM\ mut}$ together with HA-FKBP-tagged RIP3$^{RHIM\ mut}$ or RIP3^{WT} in L929 cells. We found that AP21976-induced cell death were completely comparable, regardless of whether RIP3^{WT} or RIP3$^{RHIM\ mut}$ was co-expressed with Flag-FRB*-RIP3$^{RHIM\ mut}$ (Figure 4b), suggesting that the complex containing RIP3 oligomer was not more potent than RIP3 dimer in mediating necroptosis. Similar results were also observed in *Rip3* KO cells (Figure 4c). Thus, as for necroptosis signaling *per se* RIP3 dimer and oligomer are functionally the same.

RIP3 dimerization leads to intramolecular autophosphorylation of RIP3. RIP3 is autophosphorylated in necrosome.[37,52] However, it is not clear whether RIP3 autophosphorylation is mediated by inter- or intramolecular reaction. We examined whether RIP3 was phosphorylated after dimerization with specific anti-phospho-RIP3 (T213/S232) antibody. The result showed that RIP3 dimerization led to phosphorylation on T231 or S232 (Figure 5a). There

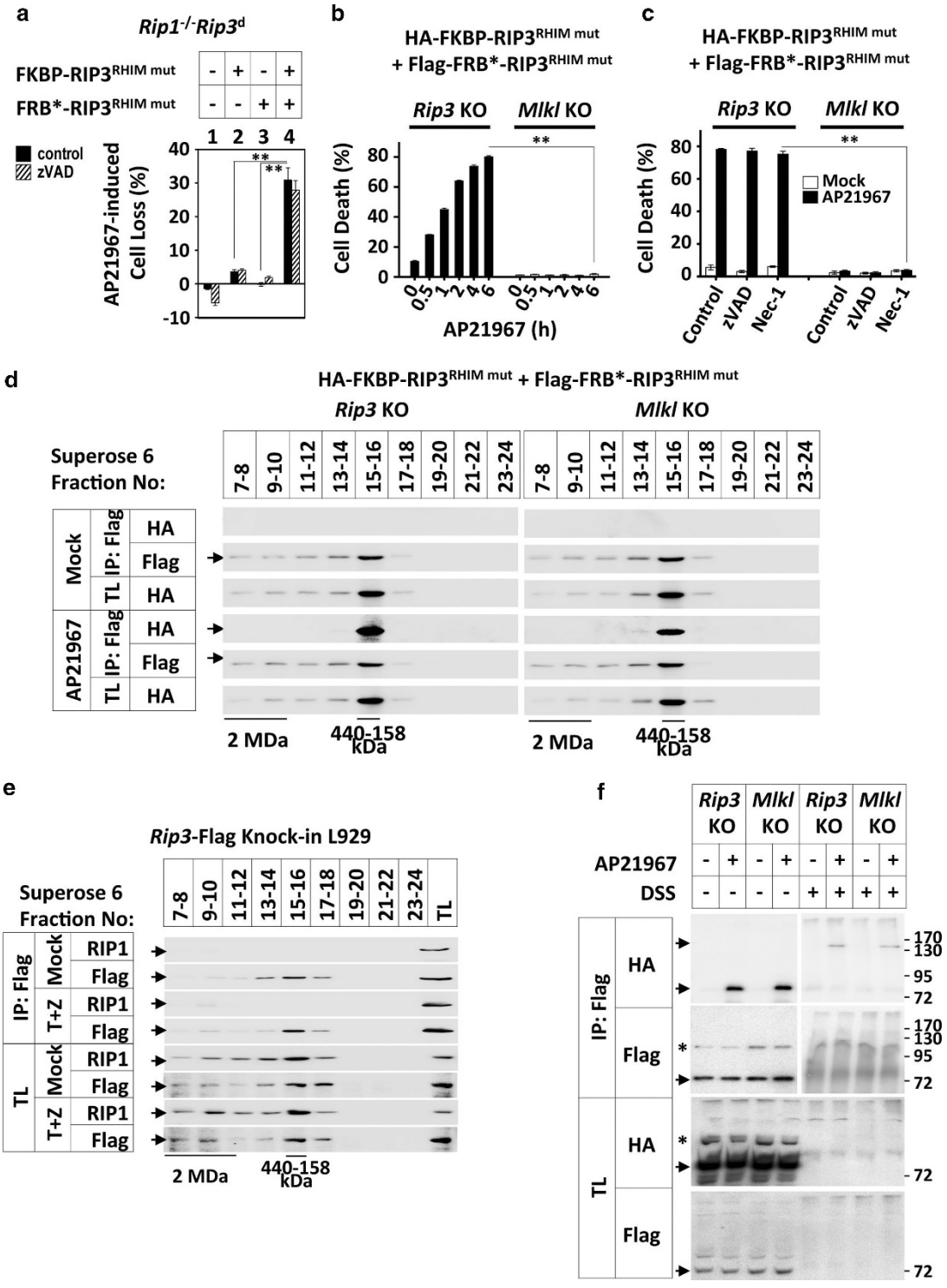

Figure 3 RIP3 homo-dimerization is sufficient to trigger MLKL-dependent necroptosis. (**a**) *Rip1*$^{-/-}$ *Rip3*^{d} MEF cells were infected with lentivirus as indicated, followed by AP21967 treatment (250 nM) for 12 h, with or without zVAD (20 μM). Cell loss was determined by ATP levels. (**b** and **c**) *Rip3* KO and *Mlkl* KO L929 cells were infected with lentivirus as indicated. Thirty-six hours post infection, these cells were treated with AP21967 (250 nM) for various time intervals (**b**), or were pretreated with DMSO, zVAD (20 uM), or necrostatin-1 (Nec-1, 30 μM) for 30 min, followed by AP21967 treatment (250 nM) for 6 h. (**c**) Cell death was determined by PI exclusion. (**d**) The cells as indicated were treated with mock or AP21967 (250 nM) for 30 min. The cell lysates were fractionated on SuperoseTM 6 size-exclusion column. These fractions were then subjected to immunoprecipitation with anti-Flag antibody, followed by western blot analysis. (**e**) The *Rip3*-Flag knock-in L929 cells were treated with mock or TNF + zVAD for 2 h. The cell lysates were fractionated as described in **d**, followed by anti-Flag immunoprecipitation and western blot analysis. (**f**) The cells as indicated were treated with mock or AP21967 (250 nM) for 30 min, followed by DSS cross-link reaction as described in Methods. The cells were then lysed and immunoprecipitated with anti-Flag antibody followed by western blotting with anti-HA antibody. Western blotting of immunoprecipitates with anti-Flag antibody shows the equal immunoprecipitation of different samples. Western blotting of total cell lysates shows equal samples used in the immunoprecipitation. All data above were represented as mean ± S.E.M. of three independent experiments. $^{**}P<0.01$

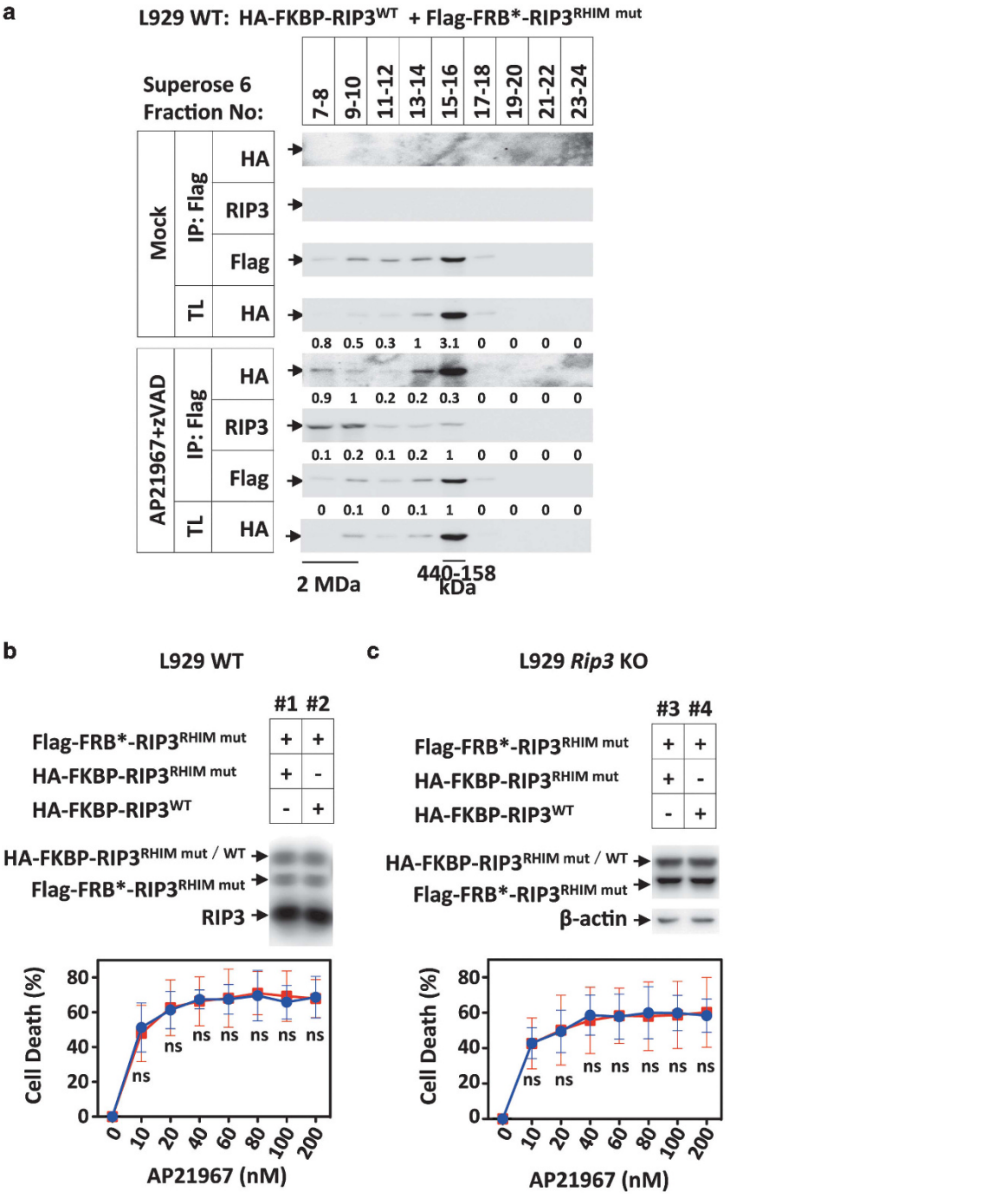

Figure 4 Oligomerization of RIP3 is not more potent than dimerization of RIP3 in generating necroptosis signaling. (**a**) Wild-type L929 cells were infected with lentivirus encoding the RIP3 variants as indicated for 24 h. After mock or AP21967 + zVAD treatment for 30 min, the cell lysates were fractionated and immunoprecipitated as described in Figure 3d, followed by western blotting analysis. The relative levels of protein were calculated by Image J and indicated. (**b** and **c**) Wild-type and *Rip3* KO L929 cells were infected with lentivirus encoding the RIP3 variants as indicated. After 24 h, these cells were re-plated and treated with AP21967 as indicated concentrations for 6 h. The protein expression was determined by western blot analysis and the cell death was determined by ATP levels. The data were represented as mean ± 95% confidence interval (CI) of three independent experiments. n.s., nonsignificant

was no phosphorylation in kinase dead mutant (D143N), but normal phosphorylation on the kinase normal partner in AP21967-induced homodimer (Figure 5b, lanes 1–8), indicating that the autophosphorylation in homodimer is mediated by intramolecular reaction. As induced RIP1–RIP3 interaction triggers RIP3 dimerization (Figure 2g), we also determined the phosphorylation of T231/S232 on RIP3 within hetrodimer, and found that only WT RIP3, but not RHIM mutant, was phosphorylated (Supplementary Figure S2e). This autophosphorylation is independent of MLKL, because similar results were also observed in *Mlkl* KO cells (Figure 5b, lanes 13–20). The specificity of anti-phospho-RIP3

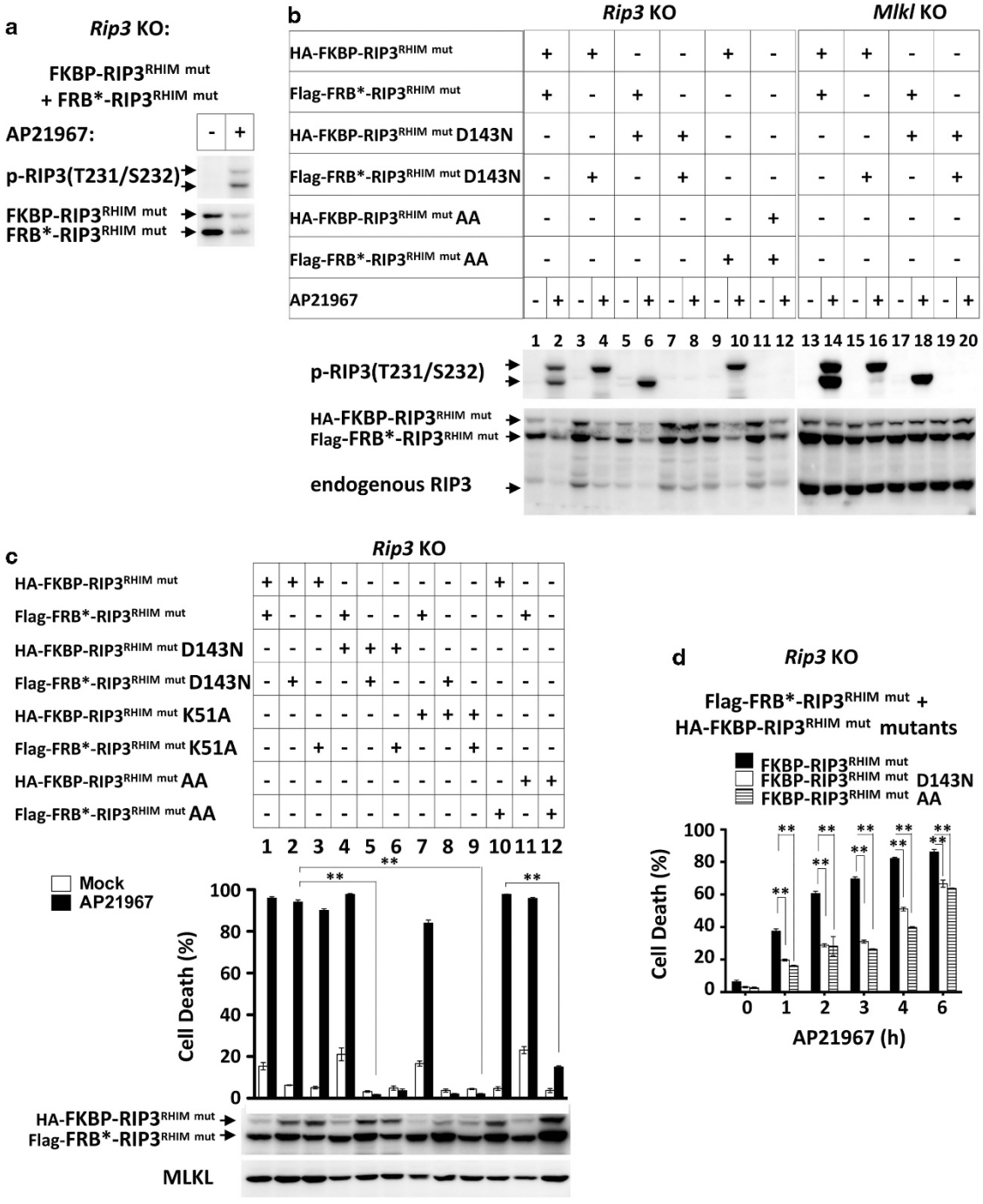

Figure 5 RIP3 homo-dimerization triggers intramolecular autophosphorylation. (**a**) The *Rip3* KO L929 cells, expressing the indicated RIP3 variants, were treated with AP21967 (250 nM) for 30 min. The cell lysates were analyzed by western blotting with antibodies as indicated. (**b**–**d**) *Rip3* KO and *Mlkl* KO L929 cells were infected with lentivirus as indicated. Thirty-six hours post infection, these cells were treated with mock or AP21967 (250 nM) for 30 min (**b**), or 6 h (**c**), or as indicated (**d**). AA represents T231A/S232A mutation. The cell lysates were analyzed by western blotting. The cell death was determined by PI exclusion. All data above were represented as mean ± S.E.M. of three independent experiments. $^{**}P < 0.01$

antibody was determined by the phosphorylation sites mutant (T231A/S232A, indicated as AA) (Figure 5b, lanes 9–12). WT RIP3 was still able to undergo autophosphorylation when it dimerized with RIP3 (AA) mutant (Figure 5b, lanes 9 and10). Collectively, our data demonstrate that RIP3 autophosphorylation is an intramolecular reaction and independent of MLKL.

It is known that RIP3's kinase activity and autophosphorylation are required for necroptosis.[52] However, it is not clear whether the loss of kinase activities or T231/S232 phosphorylations in one or some RIP3 protein molecules in necrosome would affect necroptosis signaling. We co-expressed FKBP and FRB*-tagged RIP3$^{RHIM\ mut}$ containing no mutation, K51A (kinase dead) or D143N (kinase dead) mutation, or AA

mutation with different combinations in *Rip3* KO L929 cells, and measured AP21967-induced necroptosis. We found that although one kinase dead RIP3 in a dimer blocked its own phosphorylation, as long as the other RIP3 in the dimer has kinase activity, the dimer is still capable to induce necroptosis (Figure 5c, lanes 1–4 and 7). Only the loss of the kinase activity of both RIP3 molecules in homodimer led to complete loss of the function of triggering necroptosis (Figure 5c, lanes 5–6 and 8–9). Similar results were observed when AA mutant was used (Figure 5c, lanes 10–12). Further time course experiments showed that defect in kinase activity or auto-phosphorylation of one RIP3 in dimer attenuated dimer-induced necroptosis (Figure 5d). Thus, not all RIP3 in necrosome need to be active to trigger necroptosis, but the kinase activity mediated autophosphorylation of each RIP3 protein has additive effect on triggering necroptosis.

Dimerization-mediated phosphorylation of RIP3 leads to recruitment of MLKL. To investigate whether dimerization-induced phosphorylation of RIP3 is required for MLKL recruitment, we co-expressed FKBP and FRB*-tagged $RIP3^{RHIM\ mut}$ in L929 cells and treated the cells with or without AP21967. The co-immunoprecipitation results showed that MLKL was detected in the immunoprecipitates

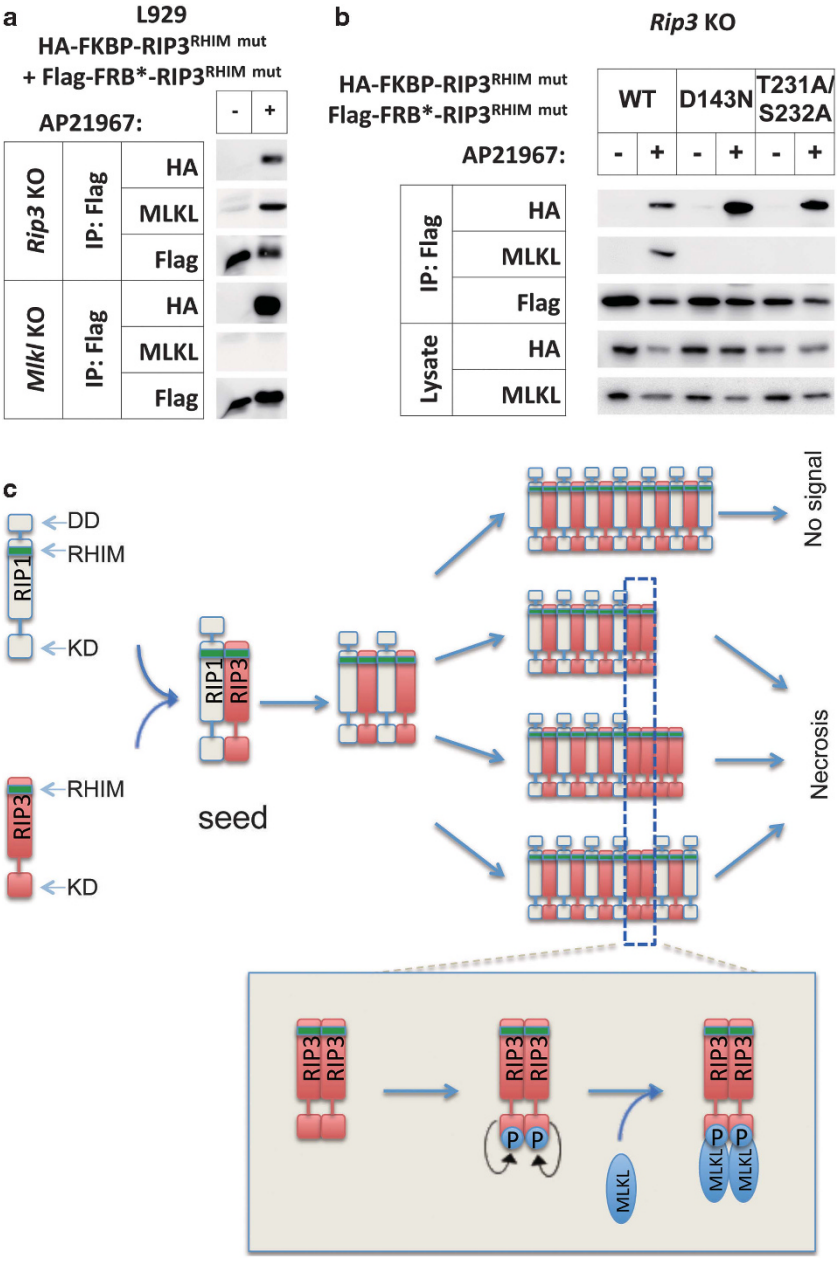

Figure 6 RIP3 homo-dimerization leads to MLKL recruitment. (**a** and **b**) *Rip3* KO and *Mlkl* KO L929 cells were infected with lentivirus as indicated. Thirty-six hours post infection, these cells were treated with mock or AP21967 (250 nM) for 30 min. The cell lysates were immunoprecipitated with anti-Flag antibody and then analyzed by western blotting. (**c**) Proposed model of signaling events in necrosome

of RIP3 dimer in *Rip3* KO but not in control *Mlkl* KO cells (Figure 6a). We next tested whether D143N or AA mutation would affect the recruitment of MLKL and found that neither the dimer of kinase dead mutant nor that of phosphorylation site mutant could recruit MLKL (Figure 6b). Thus, RIP3 dimerization mediated autophosphorylation of RIP3 is required for MLKL to be recruited to RIP3 complex.

Discussion

It is known that necrosome is an MDa complex. Although the other necrosome components such as FADD and caspase-8 contribute to the size of necrosome, the amyloid complex of RIP1 and RIP3 should be the core of necrosome. It is known that RHIM domain in RIP1 and RIP3 mediates polymerization of RIP1 and RIP3 to form heterodimeric amyloid scaffold, which provides a platform for signaling reactions to occur in necrosome.[47] However, the role of RIP1–RIP3 hetero- and RIP3–RIP3 homo-interaction, order of the signaling events and how the signaling proteins organized on the amyloid scaffold is still important to know. Based on the data presented in this report, we proposed a model shown in Figure 6c. The upstream signal leads to the formation of RIP1–RIP3 heterodimer, which functions as seeds to form heterodimeric amyloid scaffold; the interaction with RIP1 enables RIP3 in the end of the scaffold fibril to recruit other free RIP3; the RIP3–RIP3 interaction leads to RIP3 intramolecular autophosphorylation; the phosphorylated RIP3 recruits MLKL for subsequent execution of necroptosis.

The polymerization potential of RHIM *in vitro* suggests that RIP1 and/or RIP3 could be polymerized in a random manner. The RIP1–RIP3 heterodimer could be a seed for filamentous complex formation.[47] As the formation of hetero-oligomeric fibrils is more optimal (with Ile-Val contacts) than homo-oligomeric complex of RIP1 or RIP3 (with Ile-Ile or Val-Val contacts) as predicted by structural studies,[47] the necrosome scaffold is likely to be primarily RIP1–RIP3 heterodimeric amyloid. As RIP1–RIP3 interaction by itself cannot propagate necroptosis signaling (Figure 2), the RIP1–RIP3 portion of the scaffold is unlikely to transduce signaling downstream. As RIP3–RIP3 homodimerization but not RIP1–RIP1 or RIP1–RIP3 dimerization is responsible for downstream necroptosis signaling (Figures 2 and 3), and we showed that interaction with RIP1 allows RIP3 to become capable of recruiting other free RIP3 (Figure 2g), recruitment of RIP3 to the RIP3 in the scaffold should be the next signaling step after RIP1–RIP3 complex formation. Because of the higher affinity of RIP1–RIP3 interaction than that of RIP3–RIP3 interaction, high concentration of free RIP3 would favor the recruitment of RIP3 by the RIP3 in the scaffold and high level of RIP1 could have a negative effect. This prediction is consistent with Oberst group's data that RIP1 has both positive and negative role in RIP3-mediated necroptosis.[55] As the potency of RIP3 dimer is not less than RIP3 oligomer in inducing necroptosis (Figure 4), there is not a functional requirement of forming RIP3 oligomers, although RIP3 by itself can do so *in vitro*.[47] If RIP3–RIP3 dimer was considered as function unit, the number of this unit, rather than whether this unit is continuously linked together (homopolyer) or randomly distributed in RIP1–RIP3 heterodimeric polymer, is important for necroptosis signaling. The size of necrosome may not be important for necroptosis signaling, as artificial dimerization of RIP3 is sufficient to trigger necroptosis. It has been reported that defect in RIP3 phosphorylation or depletion of MLKL caused massive RIP3 aggregation,[52] suggesting that recruitment of MLKL actually prevents the RIP3 homo-interaction from forming large molecular weight aggregates. Thus, the amyloid structure in necrosome should be tightly controlled and the signaling events on the amyloid scaffold in necrosome should be organized.

The assembly of highly oligomeric signalosomes has been proposed to be an emerging principle in signal transduction.[47] Compared with other oligomeric scaffold such as DD domain-mediated oligomers, RHIM domain appears to be more capable in oligomerization (Figure 1), but the impact of such ability on signal transduction is unclear. Our data suggests that high-order oliogmerization is not indispensable for necroptosis signaling, although a platform for protein–protein interaction is absolutely required for signaling to necroptosis. Published studies have already demonstrated that specific scaffold is required for accurate signaling transduction such as DD for apoptosis and RHIM for necroptosis. Our data reported here may decipher the functional units in supramolecular necrosome and open fresh perspectives for signaling within this complex.

Materials and Methods

Cells. *Rip1*$^{-/-}$ *Rip3*^{d} MEF was renamed from *Rip1*$^{-/-}$ MEF as described,[5] as RIP3 protein cannot be detected in this cell line. Human embryonic kidney 293T cells and mouse fibroblast L929 cells were obtained from American Type Culture Collection. *Rip3* KO and *Mlkl* KO L929 cell lines were generated using TALE-nucleases methods as described.[52] RIP3-Flag knock-in L929 cells were generated by inserting Flag-tag coding sequence downstream of *Rip3* gene on genome using recombination methods, followed by verification using genomic PCR and western blotting.

DNA constructs. Plasmids used as templates containing FK506-binding protein domain (FKBP) and the mutant FRB domain (FRB*) were obtained from ARGENT Regulated Heterodimerization Kit kindly provided by ARIAD Pharmaceuticals (Cambridge, MA, USA; now iDimerize Inducible Heterodimer System by Clontech, Palo Alto, CA, USA). To generate the target fusion constructs, FKBP, FRB* (T2098L), HBD* (G521R), murine RIP1$^{RHIM\ mut}$ (QIG529-531AAA), RIP3$^{RHIM\ mut}$ (QIG449-451AAA), and RIP3 were amplified by standard PCR and cloned into the lentiviral vector pBOBI using the Exo III-assisted ligase-free cloning method. D143N, K51A, and T231A/S232A mutation RIP3 were introduced by two-round PCR. All plasmids were verified by DNA sequencing.

Reagents. AP21967 (now A/C Heterodimerizer) was obtained from ARIAD Pharmaceuticals. Benzyloxycarbonyl-Val-Ala-Aspfluoromethylketone (zVAD) was obtained from Calbiochem (San Diego, CA, USA). 4-Hydroxytamoxifen and propidium iodide were from Sigma (St. Louis, MO, USA). Necrostatin-1 (Nec-1) was provided by EMD Chemicals (Gibbstown, NJ, USA). Murine TNFα was purchased from eBioscience (San Diego, CA, USA). DSS was obtained from Thermo Scientific Pierce Biotechnology (Rockford, IL, USA).

Cell death assay. Cell death was analyzed using FACS or CellTiter-Glo Luminescent Cell Viability Assays kit (Promega, Madison, WI, USA). FACS analysis was performed as previously described.[5] The Luminescent Cell Viability Assays were performed according to the manufacturer's instruction. In brief, 10^5 cells were seeded in 96-well plate with white wall (Nunc). After treatment, equal volume of Cell Titer Glo reagent was added to the cell culture medium, which had been equilibrated to room temperature for 30 min, cells were shacked for 5 min and incubated at room temperature for 15 min. Luminescent recording was performed with POLAR star Omega (BMG Labtech, Durham, NC, USA). The % of cell loss was determined by % of ATP loss. The ATP amount of

AP21967-treated sample was normalized to that of mock-treated sample, which was regarded as 100%. When zVAD was present, the ATP amount of AP21967 + zVAD-treated sample was normalized to that of zVAD-treated sample, which was regarded as 100%. Results are presented as the mean ± S.E.M. or 95% CI of three independent experiments.[56] Comparisons were performed with a two-tailed Student's *t*-test.

Antibodies. Mouse anti-Flag M2 and anti-Myc antibodies/beads were obtained from Sigma. Rabbit anti-HA (Y-11) antibody and mouse anti-β-actin (C4) antibody were obtained from Santa Cruz Biotechnology (Santa Cruz, CA, USA). Mouse anti-RIP1 antibody was obtained from BD Biosciences (San Jose, CA, USA). The anti-phospho-RIP3 (T231/S232) and anti-MLKL antibodies were generated as described.[52]

Lentivirus preparation and infection. Lentivirus preparation and infection were performed as described.[5] 293T cells were co-transfected with pBOBI constructs and lentivirus-packing plasmids (PMDL/REV/VSVG) by calcium phosphate precipitation followed by changing with fresh medium after 12 h. The lentivirus-containing supernatant was collected 36 h later and used for infection with 10 μg/ml polybrene.

Treatment. Cells were treated with zVAD (20 μM), AP21967 (100 or 250 nM), Nec-1 (30 μM), DSS (2.5 mM), mouse TNF (10 ng/ml), and 4-OHT (1 μM), unless stated otherwise. Pre-treatment was performed 30 min ahead.

Immunoprecipitation. For Myc and Flag immunoprecipitation, cells were washed with ice-cold PBS and lysed in lysis buffer (20 mM Tris-HCl, pH7.5, 150 mM NaCl, 1 mM Na_2EDTA, 1 mM EGTA, 1% Triton X-100, 2.5 mM sodium pyrophosphate, 1 mM β-glycerophosphate, 1 mM Na_3VO_4) supplemented with Sigma Protease Inhibitor Cocktail. The cell lysates were centrifuged at 20 000 × *g* for 30 min, and the supernants were subjected to immunoprecipitation at 4 °C overnight. After the immunoprecipitation, the beads were washed three times in lysis buffer and the immunoprecipitated proteins were subsequently analyzed by western blotting.

DSS cross-linking. After three times wash with ice-cold PBS, the resuspended cells were cross-linked in PBS buffer containing 2.5 mM DSS for 30 min at room temperature. Cross-link reactions were quenched by suspending the cells in RIPA lysis buffer (20 mM Tris-HCl (pH 7.5), 150 mM NaCl, 1 mM Na_2EDTA, 1 mM EGTA, 1% NP-40, 1% sodium deoxycholate, 2.5 mM sodium pyrophosphate, 1 mM β-glycerophosphate, 1 mM Na_3VO_4, 0.1% SDS, and Sigma Protease Inhibitor Cocktail). The immunoprecipitation were carried out as described above.

Superose 6 Gel filtration. Gel filtration was performed on Superose 6 10/300 GL size-exclusion column and an AKTA Purifier protein purification system (GE Healthcare, Uppsala, Sweden) as described,[43,44] with minor modification. In brief, 3–4 mg lysates were separated at a flow rate of 0.4 ml/min and 2 ml fractions collected at 25 °C in PBS buffer with protease inhibitor cocktail and 1% Triton X-100 as indicated. Aliquots (100 μl) from each fraction were subjected to western blot analysis and fractions were then subjected to immunoprecipitation as described above followed by western blot analysis.

Conflict of Interest

The authors declare no conflict of interest.

Acknowledgements. We thank ARIAD Pharmaceuticals for generously providing the dimerization system. We thank Dr. Andrew Oberst for helpful discussion. This work was supported by the National Basic Research Program of China (973 Program 2013CB944903, 2014CB541804), the National Natural Science Foundation of China (31330047, 91029304, 31221065), the Hi-Tech Research and Development Program of China (863 program 2012AA02A201), the 111 Project (B12001), and the Open Research Fund of State Key Laboratory of Cellular Stress Biology, Xiamen University (SKLCSB2012KF003).

1. Vandenabeele P, Galluzzi L, Vanden Berghe T, Kroemer G. Molecular mechanisms of necroptosis: an ordered cellular explosion. *Nat Rev Mol Cell Biol* 2010; **11**: 700–714.
2. Vanden Berghe T, Vanlangenakker N, Parthoens E, Deckers W, Devos M, Festjens N *et al.* Necroptosis, necrosis and secondary necrosis converge on similar cellular disintegration features. *Cell Death Differ* 2010; **17**: 922–930.
3. Han J, Zhong CQ, Zhang DW. Programmed necrosis: backup to and competitor with apoptosis in the immune system. *Nat Immunol* 2011; **12**: 1143–1149.
4. Holler N, Zaru R, Micheau O, Thome M, Attinger A, Valitutti S *et al.* Fas triggers an alternative, caspase-8-independent cell death pathway using the kinase RIP as effector molecule. *Nat Immunol* 2000; **1**: 489–495.
5. Zhang DW, Shao J, Lin J, Zhang N, Lu BJ, Lin SC *et al.* RIP3, an energy metabolism regulator that switches TNF-induced cell death from apoptosis to necrosis. *Science* 2009; **325**: 332–336.
6. He S, Wang L, Miao L, Wang T, Du F, Zhao L *et al.* Receptor interacting protein kinase-3 determines cellular necrotic response to TNF-alpha. *Cell* 2009; **137**: 1100–1111.
7. Cho YS, Challa S, Moquin D, Genga R, Ray TD, Guildford M *et al.* Phosphorylation-driven assembly of the RIP1-RIP3 complex regulates programmed necrosis and virus-induced inflammation. *Cell* 2009; **137**: 1112–1123.
8. Rebsamen M, Heinz LX, Meylan E, Michallet MC, Schroder K, Hofmann K *et al.* DAI/ZBP1 recruits RIP1 and RIP3 through RIP homotypic interaction motifs to activate NF-kappaB. *EMBO Rep* 2009; **10**: 916–922.
9. Robinson N, McComb S, Mulligan R, Dudani R, Krishnan L, Sad S. Type I interferon induces necroptosis in macrophages during infection with Salmonella enterica serovar Typhimurium. *Nat Immunol* 2012; **13**: 954–962.
10. Sahaboglu A, Paquet-Durand O, Dietter J, Dengler K, Bernhard-Kurz S, Ekstrom PA *et al.* Retinitis pigmentosa: rapid neurodegeneration is governed by slow cell death mechanisms. *Cell Death Dis* 2013; **4**: e488.
11. Upton JW, Kaiser WJ, Mocarski ES. Virus inhibition of RIP3-dependent necrosis. *Cell Host Microbe* 2010; **7**: 302–313.
12. Duprez L, Takahashi N, Van Hauwermeiren F, Vandendriessche B, Goossens V, Vanden Berghe T *et al.* RIP kinase-dependent necrosis drives lethal systemic inflammatory response syndrome. *Immunity* 2011; **35**: 908–918.
13. Gunther C, Martini E, Wittkopf N, Amann K, Weigmann B, Neumann H *et al.* Caspase-8 regulates TNF-alpha-induced epithelial necroptosis and terminal ileitis. *Nature* 2011; **477**: 335–339.
14. Welz PS, Wullaert A, Vlantis K, Kondylis V, Fernandez-Majada V, Ermolaeva M *et al.* FADD prevents RIP3-mediated epithelial cell necrosis and chronic intestinal inflammation. *Nature* 2011; **477**: 330–334.
15. Lukens JR, Vogel P, Johnson GR, Kelliher MA, Iwakura Y, Lamkanfi M *et al.* RIP1-driven autoinflammation targets IL-1alpha independently of inflammasomes and RIP3. *Nature* 2013; **498**: 224–227.
16. Vince JE, Wong WW, Gentle I, Lawlor KE, Allam R, O'Reilly L *et al.* Inhibitor of apoptosis proteins limit RIP3 kinase-dependent interleukin-1 activation. *Immunity* 2012; **36**: 215–227.
17. Lin J, Li H, Yang M, Ren J, Huang Z, Han F *et al.* A role of RIP3-mediated macrophage necrosis in atherosclerosis development. *Cell Rep* 2013; **3**: 200–210.
18. Linkermann A, Brasen JH, Himmerkus N, Liu S, Huber TB, Kunzendorf U *et al.* Rip1 (receptor-interacting protein kinase 1) mediates necroptosis and contributes to renal ischemia/reperfusion injury. *Kidney Int* 2012; **81**: 751–761.
19. Oberst A, Dillon CP, Weinlich R, McCormick LL, Fitzgerald P, Pop C *et al.* Catalytic activity of the caspase-8-FLIP(L) complex inhibits RIPK3-dependent necrosis. *Nature* 2011; **471**: 363–367.
20. Kaiser WJ, Upton JW, Long AB, Livingston-Rosanoff D, Daley-Bauer LP, Hakem R *et al.* RIP3 mediates the embryonic lethality of caspase-8-deficient mice. *Nature* 2011; **471**: 368–372.
21. Zhang H, Zhou X, McQuade T, Li J, Chan FK, Zhang J. Functional complementation between FADD and RIP1 in embryos and lymphocytes. *Nature* 2011; **471**: 373–376.
22. Galluzzi L, Kepp O, Kroemer G. FADD: an endogenous inhibitor of RIP3-driven regulated necrosis. *Cell Res* 2011; **21**: 1383–1385.
23. Zhang DW, Zheng M, Zhao J, Li YY, Huang Z, Li Z *et al.* Multiple death pathways in TNF-treated fibroblasts: RIP3- and RIP1-dependent and independent routes. *Cell Res* 2011; **21**: 368–371.
24. Lu JV, Weist BM, van Raam BJ, Marro BS, Nguyen LV, Srinivas P *et al.* Complementary roles of Fas-associated death domain (FADD) and receptor interacting protein kinase-3 (RIPK3) in T-cell homeostasis and antiviral immunity. *Proc Natl Acad Sci USA* 2011; **108**: 15312–15317.
25. Moriwaki K, Chan FK. RIP3: a molecular switch for necrosis and inflammation. *Genes Dev* 2013; **27**: 1640–1649.
26. Moujalled DM, Cook WD, Okamoto T, Murphy J, Lawlor KE, Vince JE *et al.* TNF can activate RIPK3 and cause programmed necrosis in the absence of RIPK1. *Cell Death Dis* 2013; **4**: e465.
27. Thapa RJ, Nogusa S, Chen P, Maki JL, Lerro A, Andrake M *et al.* Interferon-induced RIP1/RIP3-mediated necrosis requires PKR and is licensed by FADD and caspases. *Proc Natl Acad Sci USA* 2013; **110**: E3109–E3118.
28. Chan FK, Baehrecke EH. RIP3 finds partners in crime. *Cell* 2012; **148**: 17–18.
29. Wrighton KH. Cell death: A killer puts a stop on necroptosis. *Nat Rev Mol Cell Biol* 2011; **12**: 279.
30. Wu YT, Tan HL, Huang Q, Sun XJ, Zhu X, Shen HM. zVAD-induced necroptosis in L929 cells depends on autocrine production of TNFalpha mediated by the PKC-MAPKs-AP-1 pathway. *Cell Death Differ* 2011; **18**: 26–37.

31. O'Donnell MA, Perez-Jimenez E, Oberst A, Ng A, Massoumi R, Xavier R *et al.* Caspase 8 inhibits programmed necrosis by processing CYLD. *Nat Cell Biol* 2011; **13**: 1437–1442.
32. Kim SJ, Li J. Caspase blockade induces RIP3-mediated programmed necrosis in Toll-like receptor-activated microglia. *Cell Death Dis* 2013; **4**: e716.
33. Kang TB, Yang SH, Toth B, Kovalenko A, Wallach D. Caspase-8 blocks kinase RIPK3-mediated activation of the NLRP3 inflammasome. *Immunity* 2013; **38**: 27–40.
34. Vanlangenakker N, Vanden Berghe T, Bogaert P, Laukens B, Zobel K, Deshayes K *et al.* cIAP1 and TAK1 protect cells from TNF-induced necrosis by preventing RIP1/RIP3-dependent reactive oxygen species production. *Cell Death Differ* 2011; **18**: 656–665.
35. Xie T, Peng W, Yan C, Wu J, Gong X, Shi Y. Structural insights into RIP3-mediated necroptotic signaling. *Cell Rep* 2013; **5**: 70–78.
36. Murphy JM, Czabotar PE, Hildebrand JM, Lucet IS, Zhang JG, Alvarez-Diaz S *et al.* The pseudokinase MLKL mediates necroptosis via a molecular switch mechanism. *Immunity* 2013; **39**: 443–453.
37. Sun L, Wang H, Wang Z, He S, Chen S, Liao D *et al.* Mixed lineage kinase domain-like protein mediates necrosis signaling downstream of RIP3 kinase. *Cell* 2012; **148**: 213–227.
38. Zhao J, Jitkaew S, Cai Z, Choksi S, Li Q, Luo J *et al.* Mixed lineage kinase domain-like is a key receptor interacting protein 3 downstream component of TNF-induced necrosis. *Proc Natl Acad Sci USA* 2012; **109**: 5322–5327.
39. Wu X, Tian L, Li J, Zhang Y, Han V, Li Y *et al.* Investigation of RIP3-dependent protein phosphorylation by quantitative phosphoproteomics. *Mol Cell Proteomics* 2012; **11**: 1640–1651.
40. Kaiser WJ, Sridharan H, Huang C, Mandal P, Upton JW, Gough PJ *et al.* Toll-like Receptor 3-mediated Necrosis via TRIF, RIP3, and MLKL. *J Biol Chem* 2013; **288**: 31268–31279.
41. Murphy JM, Lucet IS, Hildebrand JM, Tanzer MC, Young SN, Sharma P *et al.* Insights into the evolution of divergent nucleotide-binding mechanisms among pseudokinases revealed by crystal structures of human and mouse MLKL. *Biochem J* 2013; **457**: 369–377.
42. Zhou Z, Han V, Han J. New components of the necroptotic pathway. *Protein Cell* 2012; **3**: 811–817.
43. Feoktistova M, Geserick P, Kellert B, Dimitrova DP, Langlais C, Hupe M *et al.* cIAPs block Ripoptosome formation, a RIP1/caspase-8 containing intracellular cell death complex differentially regulated by cFLIP isoforms. *Mol Cell* 2011; **43**: 449–463.
44. Tenev T, Bianchi K, Darding M, Broemer M, Langlais C, Wallberg F *et al.* The Ripoptosome, a signaling platform that assembles in response to genotoxic stress and loss of IAPs. *Mol Cell* 2011; **43**: 432–448.
45. Micheau O, Tschopp J. Induction of TNF receptor I-mediated apoptosis via two sequential signaling complexes. *Cell* 2003; **114**: 181–190.
46. Sun X, Yin J, Starovasnik MA, Fairbrother WJ, Dixit VM. Identification of a novel homotypic interaction motif required for the phosphorylation of receptor-interacting protein (RIP) by RIP3. *J Biol Chem* 2002; **277**: 9505–9511.
47. Li J, McQuade T, Siemer AB, Napetschnig J, Moriwaki K, Hsiao YS *et al.* The RIP1/RIP3 necrosome forms a functional amyloid signaling complex required for programmed necrosis. *Cell* 2012; **150**: 339–350.
48. Vandenabeele P, Declercq W, Van Herreweghe F, Vanden Berghe T. The role of the kinases RIP1 and RIP3 in TNF-induced necrosis. *Sci Signal* 2010; **3**: re4.
49. Degterev A, Hitomi J, Germscheid M, Ch'en IL, Korkina O, Teng X *et al.* Identification of RIP1 kinase as a specific cellular target of necrostatins. *Nat Chem Biol* 2008; **4**: 313–321.
50. Jain A, Liu R, Ramani B, Arauz E, Ishitsuka Y, Ragunathan K *et al.* Probing cellular protein complexes using single-molecule pull-down. *Nature* 2011; **473**: 484–488.
51. Pollock R, Giel M, Linher K, Clackson T. Regulation of endogenous gene expression with a small-molecule dimerizer. *Nat Biotechnol* 2002; **20**: 729–733.
52. Chen W, Zhou Z, Li L, Zhong CQ, Zheng X, Wu X *et al.* Diverse sequence determinants control human and mouse receptor interacting protein 3 (RIP3) and mixed lineage kinase domain-like (MLKL) interaction in necroptotic signaling. *J Biol Chem* 2013; **288**: 16247–16261.
53. Littlewood TD, Hancock DC, Danielian PS, Parker MG, Evan GI. A modified oestrogen receptor ligand-binding domain as an improved switch for the regulation of heterologous proteins. *Nucleic Acids Res* 1995; **23**: 1686–1690.
54. Tait SW, Oberst A, Quarato G, Milasta S, Haller M, Wang R *et al.* Widespread mitochondrial depletion via mitophagy does not compromise necroptosis. *Cell Rep* 2013; **5**: 878–885.
55. Orozco S, Yatim N, Werner MR, Tran H, Gunja SY, Tait SWG *et al.* RIPK1 both positively and negatively regulates RIPK3 oligomerization and necroptosis. *Cell Death Differ* 2014; e-pub ahead of print 6 June 2014; doi:10.1038/cdd.2014.76.
56. Cumming G, Fidler F, Vaux DL. Error bars in experimental biology. *J Cell Biol* 2007; **177**: 7–11.

Supplementary Information accompanies this paper on Cell Death and Differentiation website (http://www.nature.com/cdd)